1.7 THE EVALUATION OF A DIAGNOSTIC WIND FIELD MODEL APPLIED TO THE URBAN CANOPY LAYER

Tao Zhan, Akula Venkatram*

University of California, Riverside

1. Introduction

Risk assessment, emergency response and certain urban planning tasks require models that can be used to estimate flow fields around urban structures (Brown, 2004). CFD models can, in principle, estimate these fields, but their computational and memory requirements can be burdensome enough to prevent their application in most situations. Under these circumstances, a diagnostic model that explicitly takes into account the major features of flow around building structures might is useful. Such a model can be combined with a Lagrangian particle dispersion model to estimate dispersion in a building complex. This is the basis of the code named QUIC (Quick Urban & Industrial Complex) dispersion modeling system developed by Los Alamos National Laboratory (LANL) and the University of Utah (Pardyjak and Brown, 2002; Williams et al., 2004).

In this paper, a diagnostic wind field model, based on the QUIC equations, is evaluated indirectly by comparing the concentrations associated with the flow produced by the model with measurements made in a tracer experiment conducted at the University of California, Riverside. This comparison is based on the hypothesis that dispersion in the midst of buildings is more dependent on the mean flow field than the turbulence. This paper examines this hypothesis through sensitivity studies with different turbulence parameterizations.

*Corresponding Author Address: Akula Venkatram, Department of Mechanical Engineering, University of California, Riverside, CA 92521, venky@engr.ucr.edu

2. Model Description

The model first generates the initial mean flow field (Pardyjak and Brown, 2002) by empirical specification of the flows associated with the components of the building structure. We illustrate this by considering the flow approaching an isolated cubic obstacle. In this case, the flow field can be divided into three characteristic regions called the frontal zone, the cavity zone and the wake zone (Kaplan and Dinar, 1996; also see Figure 1).

The length of the frontal zone, L_F, is calculated from

$$\frac{L_F}{H} = \frac{2(W/H)}{1+0.8(W/H)} \tag{1}$$

where W and H are the width and the height of the obstacle.

The length of the cavity zone, L_C, is specified as

$$\frac{L_C}{H} = \frac{1.8(W/H)}{(L/H)^{0.3}(1+0.24(W/H))} \tag{2}$$

where L is the length of the obstacle.

The length of the wake zone, L_W, is taken to be three times the length of the cavity zone:

$$L_W = 3L_C \tag{3}$$

The frontal zone is described by the volume bounded by the surface:

$$\frac{(x-x_{\mathrm{L}})^2}{L_{\mathrm{F}}^2(1-(z/(0.6H))^2)}+\frac{(y-y_{\mathrm{L,C}})^2}{(W/2)^2}=1 \quad (4)$$

where x_{L} is the x co-ordinate of the leftmost wall of the obstacle, and $y_{\mathrm{L,C}}$ is the y co-ordinate of the center of the leftmost wall of the obstacle.

The cavity zone is described by the volume bounded by the surface:

$$\frac{(x-x_{\mathrm{R}})^2}{L_{\mathrm{C}}^2(1-(z/H)^2)}+\frac{(y-y_{\mathrm{R,C}})^2}{(W/2)^2}=1 \quad (5)$$

where x_{R} is the x co-ordinate of the rightmost wall of the obstacle, and $y_{\mathrm{R,C}}$ is the y co-ordinate of the center of the rightmost wall of the obstacle.

The wake zone is described by the volume bounded by the surface:

$$\frac{(x-x_{\mathrm{R}})^2}{L_{\mathrm{W}}^2(1-(z/H)^2)}+\frac{(y-y_{\mathrm{R,C}})^2}{(W/2)^2}=1 \quad (6)$$

The initial velocity in the frontal zone is set to be zero.

The velocity in the cavity zone is initialized with

$$\begin{cases}\overline{u}=-\overline{u}_{\mathrm{ref}}\left(\dfrac{z}{z_{\mathrm{ref}}}\right)^{\gamma}\left(1-\dfrac{x-x_{\mathrm{R}}}{d_{\mathrm{N}}}\right)^2\\ \overline{v}=\overline{v}_{\mathrm{ref}}\left(\dfrac{z}{z_{\mathrm{ref}}}\right)^{\gamma}\\ \overline{w}=-0.5\overline{u}_{\mathrm{ref}}\left(\dfrac{z}{z_{\mathrm{ref}}}\right)^{\gamma}\left(1-\dfrac{d_{\mathrm{N}}-(x-x_{\mathrm{R}})}{0.5d_{\mathrm{N}}}\right)\end{cases} \quad (7)$$

where $\overline{u}$, $\overline{v}$ and $\overline{w}$ are the mean velocity components of the particle; $\overline{u}_{\mathrm{ref}}$ and $\overline{v}_{\mathrm{ref}}$ are the x and y components of the approach wind at the reference height z_{ref}; γ is the exponent in the power law; d_{N} is the downwind extension of the zone through the point concerned:

$$d_{\mathrm{N}}=L_{\mathrm{C}}\sqrt{\left(1-\left(\frac{z}{H}\right)^2\right)\left(1-\left(\frac{y-y_{\mathrm{R,C}}}{W/2}\right)^2\right)} \quad (8)$$

The initial velocity in the wake zone is

$$\begin{cases}\overline{u}=\overline{u}_{\mathrm{ref}}\left(\dfrac{z}{z_{\mathrm{ref}}}\right)^{\gamma}\left(1-\left(\dfrac{d_{\mathrm{N}}}{x-x_{\mathrm{R}}}\right)^{1.5}\right)\\ \overline{v}=\overline{v}_{\mathrm{ref}}\left(\dfrac{z}{z_{\mathrm{ref}}}\right)^{\gamma}\\ \overline{w}=0\end{cases} \quad (9)$$

The flow in a canyon formed between two adjacent buildings is given by

$$\begin{cases}\overline{u}=-\overline{u}_{\mathrm{ref}}\left(\dfrac{z}{z_{\mathrm{ref}}}\right)^{\gamma}\dfrac{x-x_{\mathrm{R}}}{0.5S}\dfrac{S-(x-x_{\mathrm{R}})}{0.5S}\\ \overline{v}=-\overline{v}_{\mathrm{ref}}\left(\dfrac{z}{z_{\mathrm{ref}}}\right)^{\gamma}\\ \overline{w}=-\left|0.5\overline{u}_{\mathrm{ref}}\left(\dfrac{z}{z_{\mathrm{ref}}}\right)^{\gamma}\left(1-\dfrac{x-x_{\mathrm{R}}}{0.5S}\right)\right|\\ \qquad\times\left(1-\dfrac{S-(x-x_{\mathrm{R}})}{0.5S}\right)\end{cases} \quad (10)$$

where S is the width of the canyon.

The flow fields given by equations such as (7), (9) and (10) are patched together by insisting that the final flow field is mass consistent, and at the same time is as close to the initial field as possible. This is equivalent to minimizing the functional (Sherman, 1978):

$$E(\overline{u},\overline{v},\overline{w},\lambda)= \int_V\left[\begin{array}{l}\alpha_1^2(\overline{u}-\overline{u}_0)^2+\alpha_1^2(\overline{v}-\overline{v}_0)^2\\ +\alpha_2^2(\overline{w}-\overline{w}_0)^2+\lambda\left(\dfrac{\partial\overline{u}}{\partial x}+\dfrac{\partial\overline{v}}{\partial y}+\dfrac{\partial\overline{w}}{\partial z}\right)\end{array}\right]dxdydz \quad (11)$$

where λ is the Lagrange multiplier. The subscript 0 denotes the initial fields. The constants, α_1 and α_2,

called Gaussian precision moduli, are prescribed to determine the relative importance of the adjustment of horizontal and vertical wind components. Minimization results in the set of equations relating the initial and final flow fields:

$$\begin{cases} \overline{u} = \overline{u}_0 + \dfrac{1}{2\alpha_1^2}\dfrac{\partial \lambda}{\partial x} \\ \overline{v} = \overline{v}_0 + \dfrac{1}{2\alpha_1^2}\dfrac{\partial \lambda}{\partial y} \\ \overline{w} = \overline{w}_0 + \dfrac{1}{2\alpha_2^2}\dfrac{\partial \lambda}{\partial z} \end{cases} \tag{12}$$

and the mass conservation equation:

$$\frac{\partial \overline{u}}{\partial x} + \frac{\partial \overline{v}}{\partial y} + \frac{\partial \overline{w}}{\partial z} = 0 \tag{13}$$

Substitution of Eqns. (12) into (13) yields

$$\frac{\partial^2 \lambda}{\partial x^2} + \frac{\partial^2 \lambda}{\partial y^2} + \left(\frac{\alpha_1}{\alpha_2}\right)^2 \frac{\partial^2 \lambda}{\partial z^2} = R \tag{14}$$

where R is the divergence of the initial flow field:

$$R = -2\alpha_1^2 \left(\frac{\partial \overline{u}_0}{\partial x} + \frac{\partial \overline{v}_0}{\partial y} + \frac{\partial \overline{w}_0}{\partial z} \right) \tag{15}$$

Eqns. (12) are used to adjust the initial flow field to be mass-consistent based on the field of Lagrange multipliers resulting from the solution of the partial differential equation, Eqn. (14).

Once the mean flow field is finalized, a Lagrangian scheme dispersion model uses trajectory equations to track particles released from the source (Williams et al., 2004):

$$\begin{cases} x^{t+1} = x^t + \left(\overline{u}^t + \dfrac{u'^{t+1} + u'^t}{2} \right) \mathrm{d}t \\ y^{t+1} = y^t + \left(\overline{v}^t + \dfrac{v'^{t+1} + v'^t}{2} \right) \mathrm{d}t \\ z^{t+1} = z^t + \left(\overline{w}^t + \dfrac{w'^{t+1} + w'^t}{2} \right) \mathrm{d}t \end{cases} \tag{16}$$

where the superscripts t and t+1 denote for the previous and current time point; dt is the time step; and u', v' and w' are the fluctuation velocity components of the particle.

The fluctuation velocities are updated for every time step with

$$\begin{cases} u'^{t+1} = u'^t + \mathrm{d}u' \\ v'^{t+1} = v'^t + \mathrm{d}v' \\ w'^{t+1} = w'^t + \mathrm{d}w' \end{cases} \tag{17}$$

where $\mathrm{d}u'$, $\mathrm{d}v'$ and $\mathrm{d}w'$ are the incremental changes of fluctuation velocity components.

Rodean (1996) describes a general solution to the Folker-Planck equation to calculate the incremental changes of the fluctuation velocities. Williams et al. (2004) propose a simplified version of the solution based on local co-ordinate rotation to cancel out most of the terms and the velocity gradients in the rotated co-ordinate system are used to calculate turbulent parameters.

The particle positions estimated from Eqn. (16) are converted to tracer concentrations using well known method (Williams et al., 2004).

We next describe the tracer experiment used to evaluate the model.

3. Tracer Experiment

A tracer experiment was conducted during the period of June 11th through 18th 2001 in the parking lot of College of Engineering's Center for Environmental Research and Technologies (CE-CERT) at University of California at Riverside. During the experiment, SF_6 was diluted with 10 L/min ambient air prior to dispersal and regulated at the rate of 1.4 - 5.7 g/hr from a line source mounted on top of a trailer (see Figure 2(a)). The line source consisted of fifty OD tubing with capillaries attached.

The SF_6 was sampled on two arcs at 10 m and 20 m from the source. It was also sampled at six locations all around the tracer release trailer (Figure 2(b)). All the samplers drew SF_6 at 1 m high except that at the two centerline locations, extra samplers

were used at different heights to measure the vertical concentration distribution. The SF_6 drawn by the samplers was transferred by polyethylene tubes to a trailer where the concentration was continuously analyzed. The concentrations were resolved at 5 Hz. The measured concentrations were averaged over 1 hour to compare with simulated values.

A sonic anemometer placed on top of the tracer release trailer was used to get the 'upwind' meteorological condition at the reference height of 3 m. it sampled the three components of the velocity at 10 Hz. The data of mean wind and variances were logged as 1 min averages. It was post-processed to 1 hour averages for modeling convenience. During the experiment period, the wind was predominantly westerly.

4. Model Evaluation

The model described above is used to simulate the flow field and dispersion of tracer during the tracer experiment. The computational domain is taken to be 80 m × 40 m × 11 m with a grid resolution of 1m in all three directions.

We illustrate the flow field produced by the model, by considering the meteorological conditions corresponding to the CE-CERT tracer experiment at 19:00 on 06/12/2001. In this case, the wind direction is almost westerly. The reference wind speed is 1.2 m/s at 3 m height.

In Figure 3(a), frontal zone flows and channeling effects can be seen at the upwind sides of buildings no. 1, 2, 3, 4, 7, and 11. The frontal zones for buildings no. 2, 3 and 11 can also be found in Figure 3(b). Cavity zones can be found at the downwind sides of buildings no. 2, 3, 4, and 11. A wake zone can be found at the downwind side of building no. 4. Figure 3(b) shows the existence of wake interference between buildings no. 2 and 3. Figure 3(a) shows horizontal vortices generated at both ends of the canyon between buildings no. 9 and 10, which even touch each other. This is because the canyon is short, meaning small length/height ratio. So the end effect can reach the centerline of the canyon and the flow in the canyon is substantially three-dimensional. However, since the height difference between buildings no. 9 and 10 is large (9 m for no. 9 and 1 m for no. 10), this can not be viewed as a typical regular canyon and the skimming flow regime is not resolved from a side view.

When running the dispersion model, 2400 particles are released at a constant rate over a period of 120 s. The time step for updating particle velocities and positions is taken to be 1 s. The simulated concentration corresponding to the mean flow field at 19:00 on 6/12/2001 at a height of 1 m height is shown in Figure 4(a). The wide plumes shown in the figure correspond to the flow field induced by the buildings. Some of the 'hollow' areas where the concentration should not be zero are believed to be caused by insufficient particle numbers released in the simulation.

The overall comparison between the modeled and observed concentration results is shown in ranked plot (also known as Q-Q plot) in Figure 4(b).

The results can also be presented by averaging the concentrations at each receptor and plotting it with the distance from the line source center. This allows evaluation of the spatial distribution of concentrations predicted by the model. Figure 4(c) indicates that the model over-predicts the concentration at the sampling locations around the tracer release trailer (the point at 2 m and points at 7 m distance in Figure 4(c)), where the estimated concentration is relatively high. The model is predicts well for the sampling locations at the first arc (the points at 9 - 10 m distance in Figure 4(c)). It under-predicts the concentration at the sampling locations on the second arc (the points at 19 m distance in Figure 4(c)), where the concentrations are relatively low.

To examine the hypothesis that tracer concentrations are more sensitive to the mean flow than the turbulence we simplify the turbulence parameterization included in the model described earlier (Williams et al., 2004).

We first define a turbulent velocity scale, u_T, derived from the gradients of the mean velocities in the Cartesian co-ordinate system instead of the rotated co-ordinate system used earlier

$$u_T = C_T \Delta \sqrt{\begin{aligned} &\left(\frac{\partial \overline{u}}{\partial x}\right)^2 + \left(\frac{\partial \overline{u}}{\partial y}\right)^2 + \left(\frac{\partial \overline{u}}{\partial z}\right)^2 \\ &+ \left(\frac{\partial \overline{v}}{\partial x}\right)^2 + \left(\frac{\partial \overline{v}}{\partial y}\right)^2 + \left(\frac{\partial \overline{v}}{\partial z}\right)^2 \\ &+ \left(\frac{\partial \overline{w}}{\partial x}\right)^2 + \left(\frac{\partial \overline{w}}{\partial y}\right)^2 + \left(\frac{\partial \overline{w}}{\partial z}\right)^2 \end{aligned}} \quad (18)$$

where Δ is the geometric mean of the three dimensions of the grid cell:

$$\Delta = \sqrt{\Delta x \cdot \Delta y \cdot \Delta z} \quad (19)$$

C_T is an empirically determined constant taken as 1.2.

This velocity is used to parameterize turbulent velocities based on shear layer relationships between turbulent velocities and surface friction velocity,

$$\begin{cases} \sigma_u = 2u_T \\ \sigma_v = 2u_T \\ \sigma_w = 1.3u_T \end{cases} \quad (20)$$

The velocity fluctuations are parameterized simply as

$$\begin{cases} u' = \sigma_u \mathrm{d}W_1 \\ v' = \sigma_v \mathrm{d}W_2 \\ w' = \sigma_w \mathrm{d}W_3 \end{cases} \quad (21)$$

where $\mathrm{d}W_1$, $\mathrm{d}W_2$ and $\mathrm{d}W_3$ are normally distributed random numbers with zero mean and standard deviation of 1.

Then the trajectory equation (Eqn. (16)) is used to update the particle position.

This simplified dispersion model produces concentration fields that are similar to those from the model with the more complex turbulence scheme described in Section 2. This is shown in Figure 5(a). The simplified model also over-predicts at high concentrations and under-predicts at low concentrations (Figure 5(b)). Except for the receptor right in front of the line source center, the temporally averaged concentrations at each receptor (Figure 5(c)) are similar to that by the model with complex turbulence scheme.

5. Conclusions

This study leads to the following tentative conclusions:

1. The diagnostic wind field model can capture the main features of the wind field in complex building structures.
2. A dispersion model based on the diagnostic wind field model can provide acceptable estimates of concentrations fields associated with releases in urban canopies.
3. The concentration field is relatively insensitive to turbulence parameterizations when the flow field is governed by building-induced channeling.

Acknowledgements

The research summarized in this paper was supported by the University of California Directed Research and Development (UCDRD) funding (program number RB1-014a) to collaborate with the Los Alamos National Laboratory.

We are thankful to Dr. Michael J. Brown of LANL for hosting Tao Zhan during his stay in LANL, and for his advice in developing the wind field code used in this project. We are indebted to Dr. Michael D. Williams of LANL for his help in interpreting the Lagrangian particle model.

References

Britter R.E., Hanna S.R., 2003. Flow and Dispersion in Urban Areas. Annual Review of Fluid Mechanics. 35: 469-496.

Brown M.J., 2004. Urban Dispersion – Chanllenges for Fast Response Modeling. 5th AMS Urban Environ. Conf., Vancouver, B.C.

Kaplan H., Dinar N., 1996. A Lagrangian Dispersion Model for Calculating Concentration Distribution within a Built-up Domain. Atmos. Environ. 30: 4197-4207.

Pardyjak E.R., Brown M.J., 2002. QWIC-URB v1.0 User's Guide (draft). Los Alamos National Laboratory.

Rodean H.C., 1996. Stochastic Lagrangian Models of Turbulent Diffusion. The American Meteorological Society.

Sherman C.A., 1978. A Mass-Consistent Model for Wind Fields over Complex Terrain. J. Appl. Meteor. 17: 312-319.

Williams M.D., Brown M.J., Boswell D., et al., 2004. Testing of the QUIC-PLUME Model with Wind-tunnel Measurements for a High-rise Building. 5th AMS Urban Environ. Conf., Vancouver, B.C.

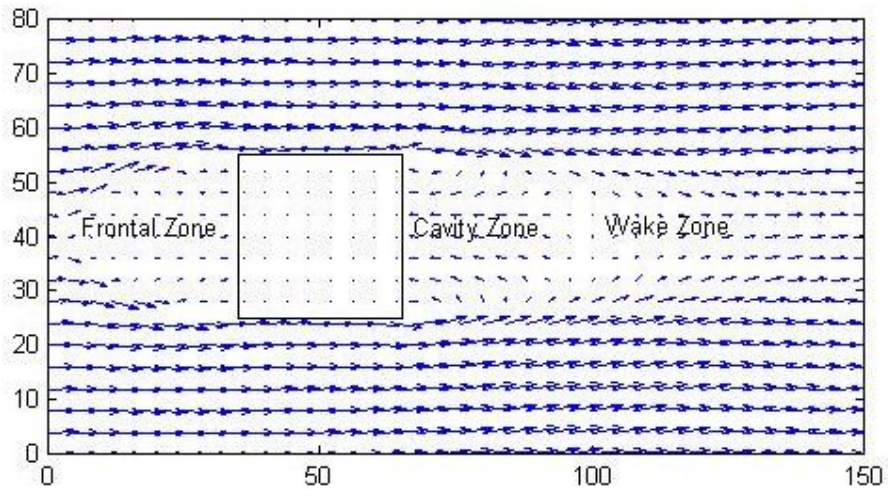

Figure 1. The three zones generated by flow approaching a single obstacle, simulated by the diagnostic flow field model described in Section 2.

(a)

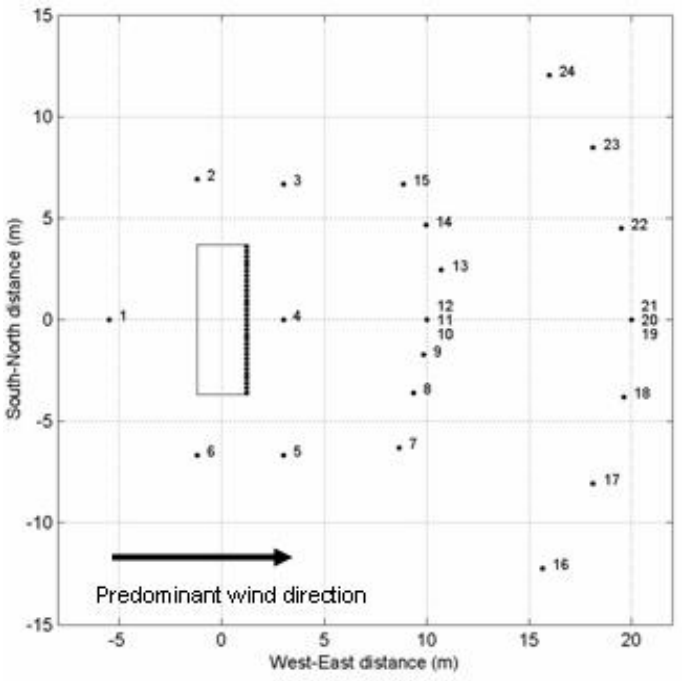

(b)

Figure 2. (a) Experimental set-up at CE-CERT parking lot, view from NW. (b) Locations of SF_6 line source (dark dotted line) and samplers.

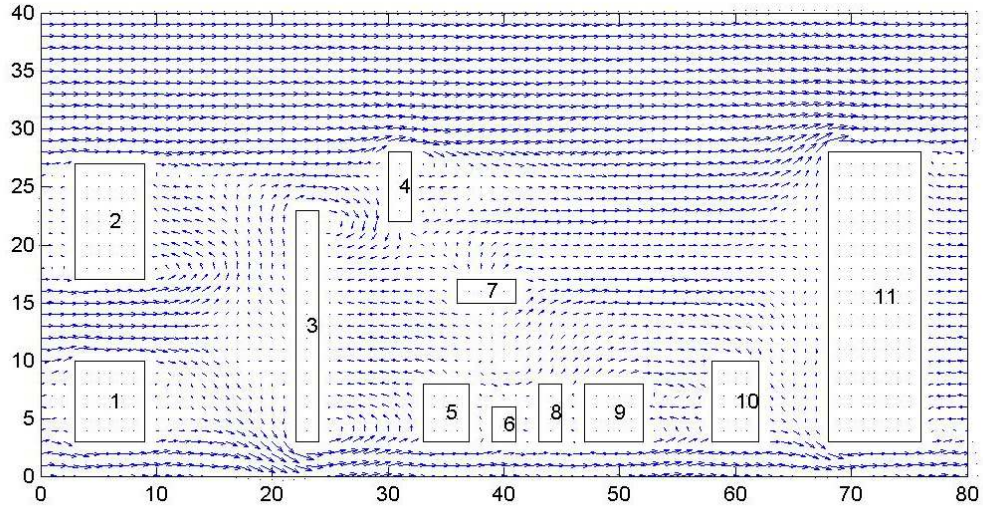

(a)

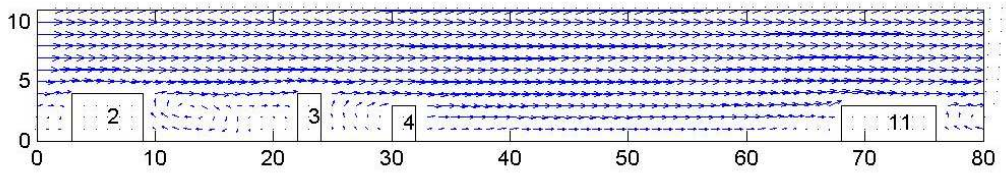

(b)

Figure 3. Flow fields after mass-consistency for case 6/12/2001 19:00. (a) Plan view at 1 m height. (b) Side view at the centerline of building no. 2.

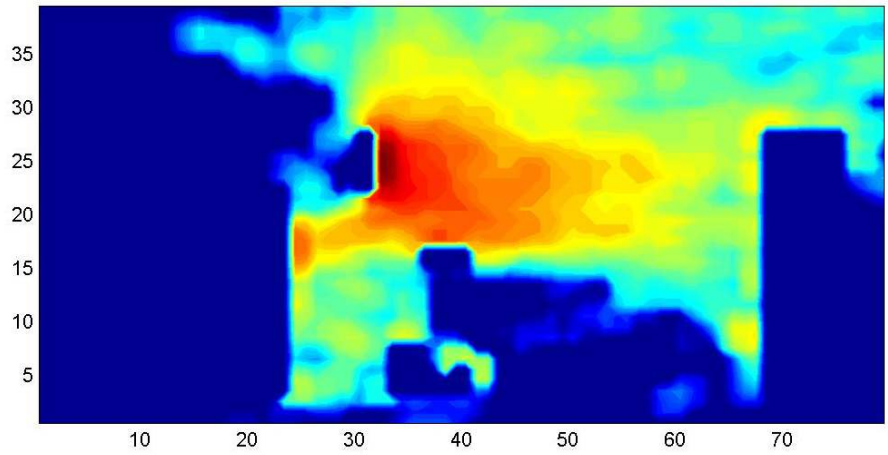

(a)

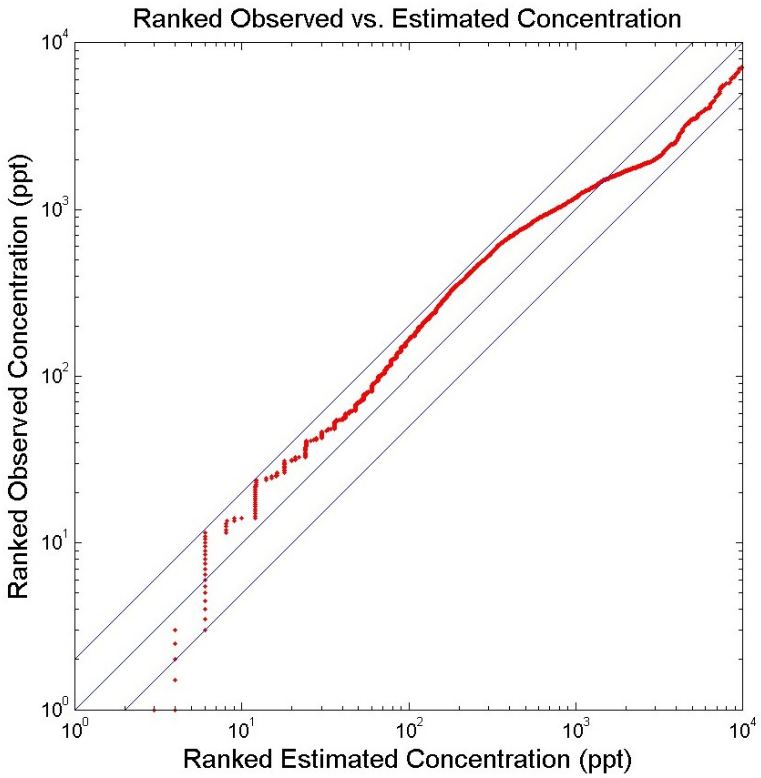

(b)

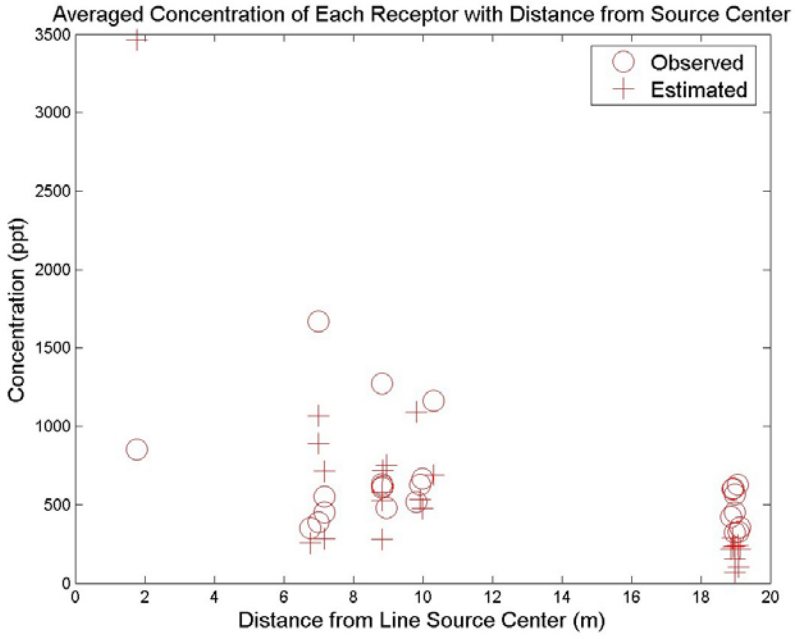

(c)

Figure 4. Concentration results with complex turbulence scheme. (a) Concentration field, 1 m height, for case 6/12/2001 19:00. (b) Ranked plot of observed vs. estimated concentrations. (c) Temporally averaged concentrations for each receptor with distance from the line source center.

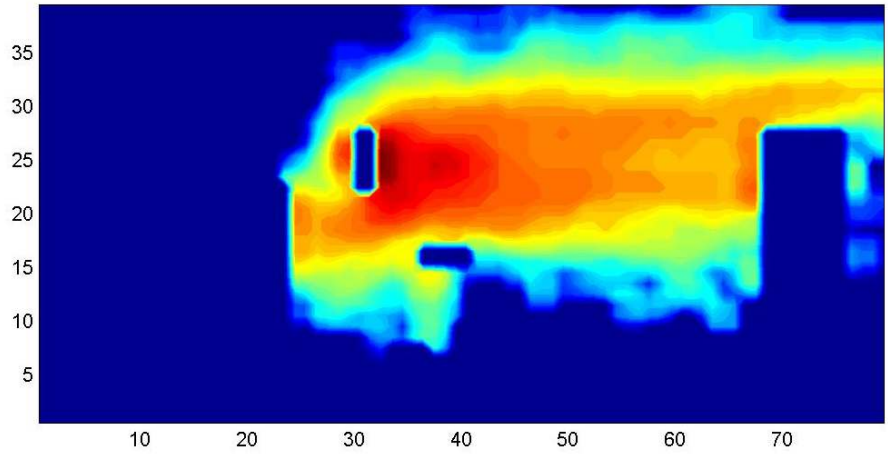
35
30
25
20
15
10
5
10
20
30
40
50
60
70

(a)

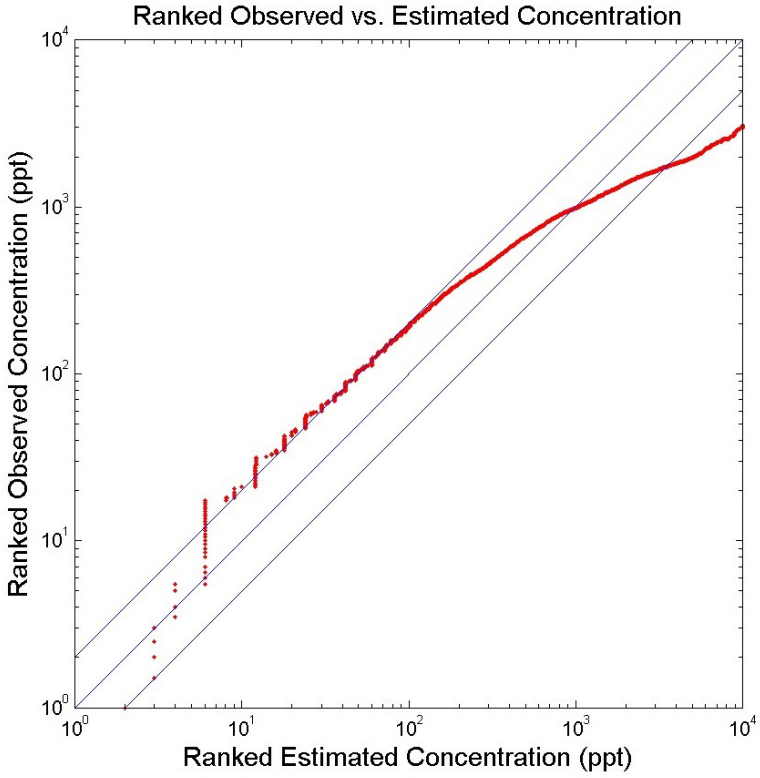
Ranked Observed vs. Estimated Concentration
Ranked Observed Concentration (ppt)
Ranked Estimated Concentration (ppt)
10^0
10^1
10^2
10^3
10^4

(b)

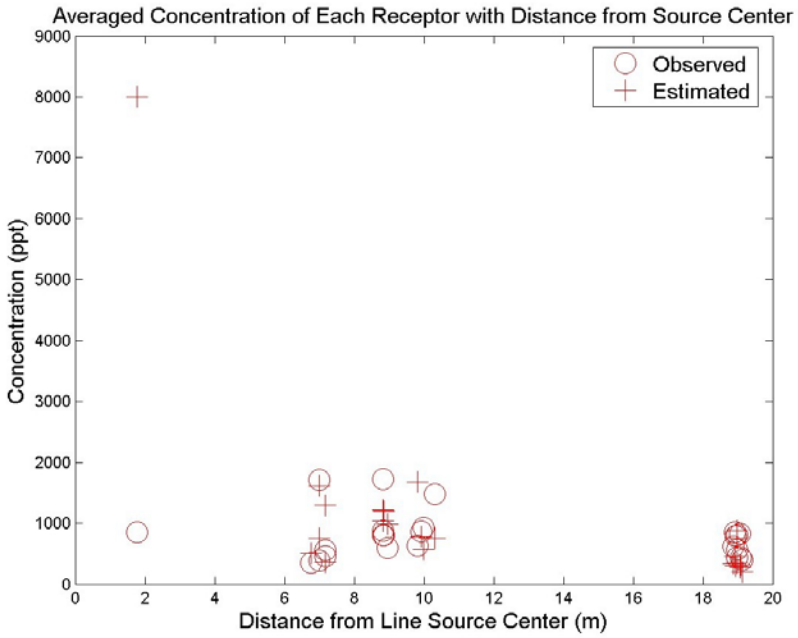

(c)

Figure 5. Concentration results with simple turbulence scheme. (a) Concentration field, 1 m height, for case 6/12/2001 19:00. (b) Ranked plot of observed vs. estimated concentrations. (c) Temporally averaged concentrations for each receptor with distance from the line source center.